ASSESSMENT OF THE RELATIONSHIP BETWEEN COLD ROLLING AND CORROSION RESISTANCE OF AZ91D MAGNESIUM ALLOY

Viviam Serra Marques Pereira, viviam.smp@gmail.com
Renato Altobelli Antunes, renato.antunes@ufabc.edu.br
Universidade Federal do ABC (UFABC), Rua Santa Adélia 166 Santo André – SP CEP: 09210-170

Mara Cristina Lopes de Oliveira, mara.oliveira@usp.br
Electrocell Ind. Com. De Equip. Elétricos LTDA – Av. Prof. Lineu Prestes 2242 Ed. CIETEC Cidade Universitária São Paulo SP CEP: 05508-000

Abstract. The aim of this work was to investigate the effect of solution treatments combined with cold rolling on the corrosion resistance of AZ91D magnesium alloy in NaCl 0.9 wt% solution at room temperature. The as-cast alloy was solution annealed at 445 ºC under non oxidizing atmosphere during 24 h and 48 h. After the solution treatment, the specimens were water quenched. Then, the specimens were cold-rolled at room temperature to 10% and 20% thickness reduction. After these steps, the microstructure of the specimens was observed by optical microscopy and SEM. The corrosion behavior was evaluated through electrochemical impedance spectroscopy and potentiodynamic polatization curves after 13 days of immersion in the electrolyte. The results showed that the solution treatment during 48 h produced the best corrosion resistance.

Keywords: AZ91D, corrosion, cold rolling

1. INTRODUCTION

Austenitic stainless steels, cobalt-chromium alloys and titanium alloys are commonly used as biomaterials for orthopaedic applications (Gallardo et al., 2004). The major limitation of these materials is the possibility of ion leaching or debris generated during corrosion and wear processes that may lead to undesirable biological reactions, reducing the biocompability of the implant device (Lothka et al., 2004; Jacobs et al., 1998; Wang et al, 1996). Another drawback of conventional metallic biomaterials is that their Young's modulus is higher than that of the human bone (typically 30 GPa). For stainless steels and cobalt-chromium alloys the Young's modulus is in the range 200 – 210 GPa (Afonso et al., 2007). For titanium alloys the Young's modulus may be as low as 60 GPa depending on the alloying elements (Hon et al., 2003). If the Young's modulus of the implant material is higher than that of the human bone the stress transfer between the implant and the osseous tissue adjacent it may be insufficient, leading to bone resorption and loosening of the biomedical device. This phenomenon is known as stress shielding effect (Azevedo and Hippert, 2002). In addition to these problems, conventional metallic implants, when used as temporary fixation devices such as plates and screws, must be removed after the healing of a fractured bone through a new surgical procedure (Park and Kim, 2003), imparting additional suffering to the patient.

In this context, research on the use of magnesium-based biomaterials has attracted growing interest. This is a consequence of the low Young's modulus of magnesium (40 GPa) that hinders the occurrence of stress shielding effect (Staiger et al., 2006). Moreover, magnesium alloys have been considered as temporary fixation implant devices due to the intrinsic biocompatibility of magnesium ions that are naturally occurring species in the human metabolism (Saris, 2000). The low chemical stability of magnesium in saline solutions such as the physiological fluid leads to a gradual deterioration. Consequently, temporary implants based on magnesium alloys would perform their mechanical function during the healing of a fractured bone. After a specific period, these devices would be absorbed by the body without the need for a surgical procedure to remove them from the patient, as occurs with conventional metallic implants. However, pure magnesium degrades too quickly. During this process, gaseous hydrogen is released at a rate that may be too high to be controlled by the human body, forming cysts (Witte et al, 2005). Thus, it is necessary to add specific alloying elements to magnesium in order to increase its chemical stability. There are successive reports on the use of magnesium alloys with Al, Zn and Mn additions as biomaterials (Zhou et al., 2010; Álvarez-Lopez et al., 2010). However, even in these cases corrosion rate may be too high. In this way, the main technological challenge is to achieve a proper control of the deterioration rate of the magnesium devices by slowing their corrosion rate. According to the literature, it is possible to control the corrosion rate of magnesium by performing suitable heat treatments that lead to the precipitation of specific crystalline phases and/or by controlling grain size through the combination of mechanical and thermal processing (Miao et al, 2009). Zhou et al. (2009) showed that aluminum-rich precipitates formed during solution annealing and ageing of AZ91D magnesium alloy played a major role in the corrosion resistance of this material. In this regard, the combination of heat treatments and cold rolling may produce structural characteristics that increase the corrosion resistance of magnesium alloys. This approach is little investigated in the literature. In this way, the aim of this work was to investigate the effect of solution treatments combined with cold rolling on the corrosion resistance of AZ91D magnesium alloy in NaCl 0.9 wt% solution at room temperature.

2. MATERIALS AND METHODS

2.1 Material

The material used in this investigation was AZ91D magnesium alloy whose nominal chemical composition is shown in Tab. 1.

Table 1.Chemical composition of AZ91D magnesium alloy.

	Al	Mn	Zn	Si	Fe	Cu	Ni	Mg
Mass (%)	8,30 – 9,70	0,15 mín.	0,35 – 1,00	0,10 máx.	0,005 máx.	0,030 máx.	0,002 máx.	Bal.

2.2 Solution annealing

Specimens of AZ91D alloy were solution annealed at 445 ºC for 24 h and 48 h under argon atmosphere followed by water quenching.

2.3 Cold rolling

After solution annealing, the specimens were cold rolled at room temperature through a single stand reversion mill. The percentages of thickness reduction were 10% and 20% obtained by successive steps of plastic deformation through the mill.

2.4 Microstructural characterization

The microstructure of AZ91D specimens was observed by optical microscopy and scanning electron microscopy (SEM). The material was observed after solution annealing and cold rolling steps. As-received (as-cast) specimens were also observed for comparison. The specimens were prepared by grinding, polishing in diamond paste and chemical etching (60 wt.% ethylene glycol, 20 wt.% glacial acetic acid and 1 wt.% nitric acid solution).

2.5 Electrochemical tests

For the polarization measurements the experimental set-up comprised a three-electrode arrangement with a platinum wire and a saturated calomel electrode (SCE) as counter and reference electrodes, respectively. A potentiostat/galvanostat Autolab PGSTAT 100 was used for the measurements. Potentiodynamic polarization curves were obtained after 13 days of immersion in NaCl 0.9 wt.% at 37 °C, using a scanning rate of 1mV s^{-1}. The potential range was from −0.5 V versus the open circuit potential (OCP) up to -0.5 V. The identification of the specimens in the legend of the figures that expose the results obtained from the electrochemical tests is based on the following example: SA 24h 10% (solution annealed for 24h and with a deformation of 10% imparted by cold rolling).

3. RESULTS AND DISCUSSION

3.1 Microstructure

The microstructure of the as-cast AZ91D alloy was observed through optical microscopy. No significant differences were observed between the specimens cold worked up to 10% or 20% of thickness reduction. In Fig. 1a an optical micrograph of the as-cast specimen is presented. The microstructure is comprised of an eutetic phase (dark, lamellar structure) embedded in the Mg-α matrix (bright). The eutetic phase consists of alternating lamellae of Mg-α and an Al-rich phase that is cathodic in relation to the matrix. This difference of potential between the eutetic phase and the Mg-α matrix may lead to the formation galvanic microcells, thus accelerating the corrosion of the matrix adjacent to the eutetic phase. This effect has been reported by several authors (Song et al., 1999; Zhao et al., 2008). A SEM micrograph of the specimen shown in Fig. 1a is presented in Fig. 1b where the eutetic phase appears as a light-gray structure within a darker matrix. The approximate composition of matrix and eutetic phases was determined by energy dispersive x-ray spectroscopy (EDS) (the spectrum is not presented). According to Zhou et al. (2009), the eutetic phase is comprised of Mg-α and β-$Mg_{17}Al_{12}$ lamellae. EDS analysis proved that the relative content of Mg and Al in this phase is close to the value reported in the literature. The analysis of the matrix showed that it consists mainly of Mg, as expected.

SEM micrographs of the solution annealed AZ91D are presented in Figs. 1c and 1d. Only micrographs of the 20%-reduced specimens that were solutionized at 445 ºC during 48 h are shown. The microstructures of the corresponding specimens that were solutionized during 24 h are very similar and were not included in the text. After solution

annealing at 445ºC for 24 and 48 h the eutetic phase was dissolved and the microstructure is comprised mainly of Mg-α matrix. This occurred for both 10% and 20% reduced specimens. Notwithstanding, some Al-rich precipitates were still present after solution treatment.
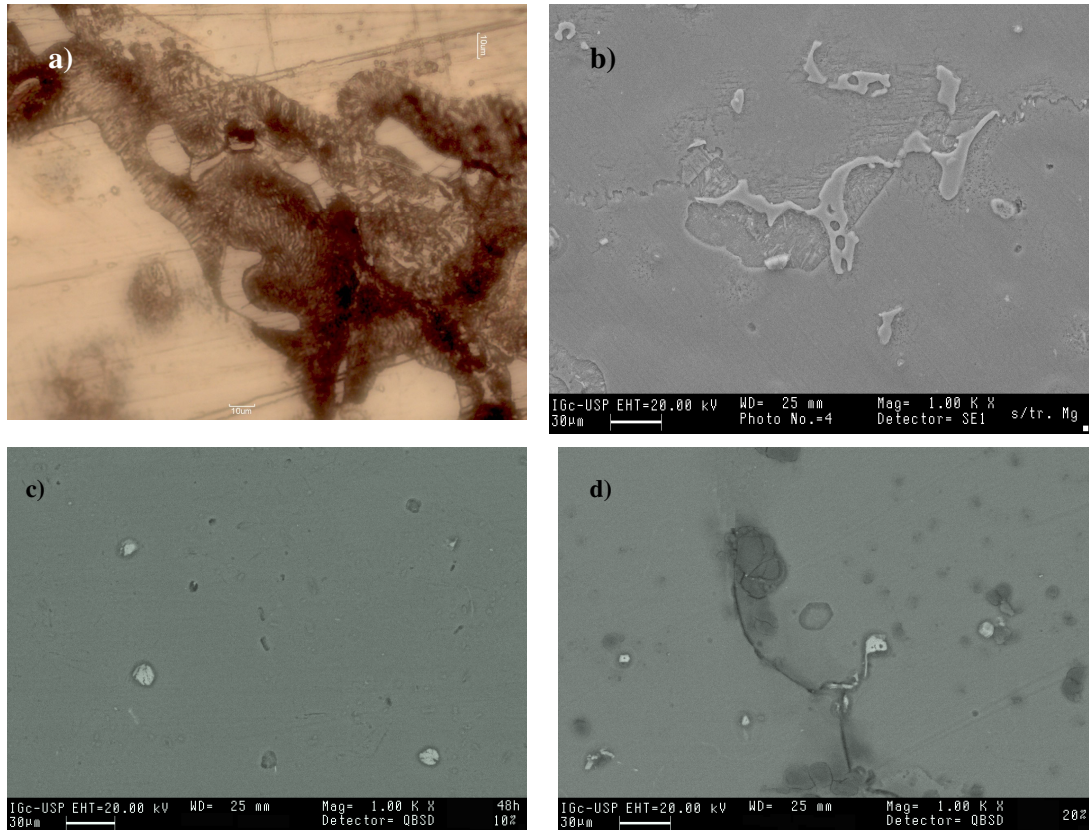

Figure 1. (a) Optical micrograph of as-cast AZ91D alloy; (b) SEM micrograph of the specimen shown in Fig. 1a.; (c) SEM micrograph of SA 48h 10% specimen; (d) SEM micrograph of SA 48h 20% specimen.

3.2 Electrochemical impedance spectroscopy (EIS)

Nyquist plots of the AZ91D subjected to different cold rolling and solution annealing conditions are shown in Fig. 2. The identification of the specimens was explained in section 2.5. The plots were obtained in NaCl 0.9 wt.% solution at 37ºC. After 1 day of immersion (Fig. 2a) the plots are comprised of a capacitive loop in the high frequency region independently of the specimen tested. In the same way, there is a well-defined inductive loop in the low frequency region for all the specimens. It is clear, then, that the heat treatment and cold rolling steps did not alter the corrosion mechanism of AZ91D. Conversely, the corrosion resistance was significantly modified as discussed below.

The high frequency capacitive loop may be attributed to corrosion processes at the electrolyte/electrode interface (Turhan et al., 2009). The presence of an inductive loop at low frequencies is frequently reported for Mg alloys (Turhan et al., 2009; Li et al., 2010). This behavior is typical of a dissolution process that metals undergo during immersion in a specific electrolyte, generating metallic ions in solution that will pass through an intermediate transition such as the formation of an adsorbed species. For Mg alloys, it is assumed that this transition is related to the formation of $Mg(OH)^+_{ads}$ and Mg^+_{ads}. As stated above the main difference between the electrochemical behaviors of the specimens was related to their corrosion resistance. The radius of the semi-circle that characterizes the capacitive loop at high frequencies has been related to charge transfer reactions at the interface specimen/electrolyte (Badawy et al., 2010). Then, impedance values associated with this semi-circle are an indication of the corrosion resistance of the specimens.
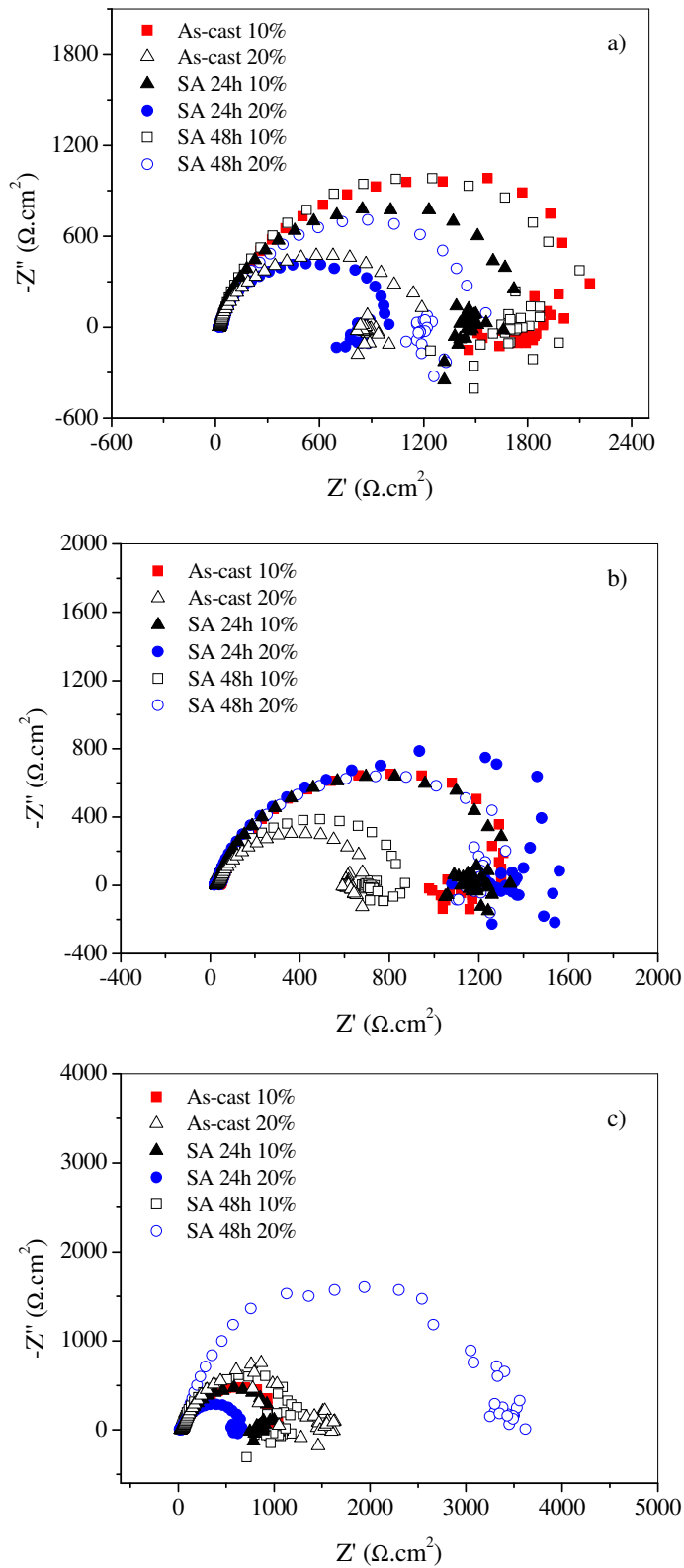
Figure 2. Nyquist plots of AZ91D alloy subjected to different conditions of solution annealing and cold rolling in NaCl 0.9 wt.% at 37ºC: a) 1 day; b) 6 days; c) 13 days of immersion.

In this context, the specimens cold rolled up to a thickness reduction of 10% presented higher impedance than the 20%-reduced specimens. This was observed for both as-cast and solution annealed materials. Moreover, the as-cast specimen presented the highest impedance, suggesting that it is the most corrosion resistant material after 1 day of immersion.

The electrochemical behavior of the AZ91D alloy after 6 days of immersion may be seen in Fig. 2b. The shape of the Nyquist plots is very similar to those obtained after 1 day of immersion (Fig. 2a). The general trend is that the impedance of all specimens decreased in comparison with the 1-day of immersion plots. Only the impedance of the specimen SA 24h 20% increased in comparison with the plot obtained after 1 day of immersion.

After 13 days (Fig. 2c) the impedance of the specimen SA 48h 20% was much higher than for the previous periods of immersion. Furthermore, the impedance of all other specimens is much lower. Impedance of the as-cast 20% specimen was higher than that of the as-cast 10% specimen. Conversely, for the specimens that were solution annealed during 24 h the impedance of the 10%-deformed material was higher than that of the 20%-deformed one. The effect of plastic deformation on the corrosion behavior of Mg-alloys is yet a subject of controversy in the literature. Some studies show that the corrosion resistance is adversely affected by metal forming processes while others show an inverse effect. Zhang et al. (2011) recently investigated the effect of hot extrusion on the corrosion resistance of AZ91 alloy. They found that the corrosion resistance decreased after extrusion. This behavior was related to the multiplication of dislocations and the formation of twins as a consequence of the plastic deformation imparted by the extrusion process. Other authors (Abuleil et al., 2009) reported an inverse trend for Mg-Sn-Ca alloys, i.e., the corrosion resistance increased after extrusion. According to the authors, recrystallization occurred during hot extrusion, leading to an increase of the grain size of the alloy. Thus, the reduction of grain boundaries accounted for the increase of corrosion resistance after extrusion.

The results obtained in this work point to a beneficial effect of deforming AZ91D to a 20% thickness reduction in the solution annealing during 48h condition. Thickness reduction was obtained by cold rolling. Hence, recrystallization during plastic deformation may be disregarded in this work. In this way, it is not likely that grain size of the Mg-α matrix increased after rolling. In fact, this could not be assessed by SEM analyses. It is likely, though, that dislocations density increased after rolling. Hence, it would be probable corrosion resistance would decrease for higher deformations. However, this expectancy was only reached by SA 24h specimens while for as-cast and SA 48h specimens the behavior was opposite to this. In this way, the discussion should encompass another important factor that has also great influence on the corrosion behavior of the alloy, that is, microstructure. As shown in Fig. 1 solution annealing dissolved β-$Mg_{17}Al_{12}$ phase. Zhou et al. (2009) reported that the solution annealed structure of AZ91D alloy may give rise to a meta-stable, partially protective film of high aluminum content on the Mg-α matrix. This film may prevent corrosion during specific periods of immersion. However, as it is meta-stable, the proactive action is lost with time. Apparently, cold rolling may help to stabilize this film for longer periods, giving rise to a high corrosion resistance. Moreover, despite the fact the grain size of the matrix was not evaluated through SEM micrographs, it is likely that it is higher for the specimens that were solution annealed during 48 h in comparison with those that were treated during only 24h further enhancing the corrosion resistance of AZ91D alloy.

3.3 Potentiodynamic polarization curves

Potentiodynamic polarization curves of AZ91D subjected to different conditions of solution annealing and cold rolling after 13 days of immersion in NaCl 0.9 wt.% at 37 ºC are shown in Fig. 3. Electrochemical parameters determined from these curves are shown in Tab. 2. Corrosion potential (E_{corr}) was little affected by either solution annealing or cold rolling operations. Corrosion current density (i_{corr}) is related to the kinetic of corrosion processes on the surface of the metallic electrode. The higher is the value of i_{corr} the lower is the corrosion resistance of the material. As seen in Tab. 2 the results are in good agreement with those obtained by EIS. SA 48h 20% presented the lowest value of i_{corr}, indicating its relative high corrosion resistance in comparison with the other specimens. Indeed, it was the only specimen that presented a self-passivating behavior with a passive current density of 3.6 $\mu A.cm^{-2}$ and a passive range between -1.21 V and -0.97 V. The specimens that were solution annealed during 24 were the least corrosion resistant for both cold reductions. After solution annealing, some residual β-$Mg_{17}Al_{12}$ phase still remained in the microstructure of the alloy as exemplified in Figs. 1a and 1b. The small cathodic are represented by the residual β-$Mg_{17}Al_{12}$ phase in comparison with the adjacent Mg-α matrix would lead to a highly localized corrosion mechanism of the anodic Mg-α that surrounds the small cathodic residual β-$Mg_{17}Al_{12}$ phase. This effect has been reported by Zhou et al. (2009) and would manifest when the meta-stable Al protective film on the Mg-α has no longer stability to prevent corrosion. As the decrease of corrosion resistance was found for the SA 24h and not for the SA 48h it is likely that the protective aluminum film would be more stable for the specimens annealed during 48h, thus accounting for their higher corrosion resistance.
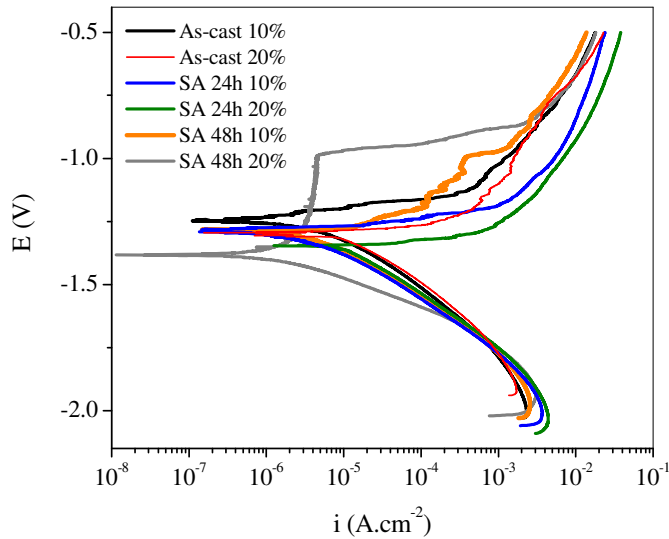
Figure 3. Potentiodynamic polarization curves of AZ91D subjected to different conditions of solution annealing and cold rolling after 13 days of immersion in NaCl 0.9 wt.% at 37 ºC.

Table 2. Electrochemical parameters obtained from the potentiodynamic polarization curves shown in Fig. 3.

	As-cast 10%	As-cast 20%	T4 24h 10%	T4 24h 20%	T4 48h 10%	T4 48h 20%
E_{corr} (V)	-1.25	-1.29	-1.28	-1.35	-1.29	-1.38
i_{corr} ($\mu A.cm^{-2}$)	1.9	4.2	3.5	16.9	3.2	1.3

4. CONCLUSIONS

Solution annealing of AZ91D alloy during 48h produced the best corrosion resistance for a 20%-cold reduction by rolling. Modifications of the microstructure of the alloy during heat treatment were directly related to the electrochemical behavior. The role of plastic deformation on the corrosion resistance could be assessed mainly as a qualitative approach. Further investigations are necessary to clarify the mechanisms that led to the increase of corrosion resistance with cold reduction.

5. ACKNOWLEDGEMENTS

6. REFERENCES

Abu Leil, T., Hort, N., Dietzel, W., Blawert, C., Huang, Y., Kainer, K.U., Rao, K.P., 2009. "Microstructure and corrosion behavior of Mg-Sn-Ca alloys after extrusion". Transactions of Nonferrous Metals China, Vol. 19, pp. 40-44.
Afonso, C.R.M., Aleixo, G.T., Ramirez, A.J. and Caram, R., 2007. "Influence of cooling rate on microstructure of Ti-Nb alloy for orthopedic implants". Materials Science and Engineering C, Vol. 27, pp. 908-913.

Alvarez-Lopez, M., Pereda, M.D., Del Valle, J.A., Fernandez-Lorenzo, M., Garcia-Alonso, M.C., Ruano, O.A. and Escudero, M.L., 2010. "Corrosion behaviour of AZ31 magnesium alloy with different grain sizes in simulated biological fluids". Acta Biomaterialia, Vol. 6, pp. 1763-1771.

Azevedo, C.R.F. and Hippert, Jr.E., 2002. "Failure analysis of surgical implants in Brazil". Engineering Failure Analysis, Vol. 9, pp. 621-633.

Badawy W.A., Hilal N.H., El-Rabiee M., Nady H., 2010. "Electrochemical behavior of Mg and some Mg alloys in aqueous solutions", Electrochimica Acta, Vol. 55, pp. 1880-1887.

Gallardo, J., Durán, A. and De Damborenea, J.J., 2004. "Electrochemical and in vitro behaviour of sol-gel coated 316L stainless steel". Corrosion Science, Vol. 46, pp. 795-806.

Hon, Y.-H., Wang, J.-Y. and Pan, Y.-N.,, 2003. "Composition/phase structure and properties of titanium-niobium alloys". Materials Transactions, Vol. 44, pp. 2384-2390.

Jacobs, J.J., Gilbert, J.L. and Urban, R.M., 1998. "Current concepts review – Corrosion of metal orthopaedic implants". Journal of Bone and Joint Surgery, Vol. 80, pp. 268-282.

Li Q., Xu S., Hu J., Zhang S., Zhong X., Yang X., 2010. "The effects to the structure and electrochemical behavior of zinc phosphate conversion coatings with ethanolamine on magnesium alloy AZ91D", Electrochimica Acta, Vol. 55, pp. 887-894.

Lothka, C., Szekeres, T., Steffan, I., Zhuber, K. and Zweymuller, K., 2003. "Four-year study of cobalt and chromium blood levels in patients managed with two different metal-on-metal total hip replacements". Journal of Orthopaedic Research, Vol. 21, pp. 189-195.

Miao, Q., Hu, L.-X., Sun, H.-F. and Wang, E.D., 2009. "Grain refining and property improvement of AZ31 Mg alloy by hot rolling". Transactions of Nonferrous Metals Society of China, Vol. 19, pp. s326-s330.

Park, J.B. and Kim, Y.K. In: Park J. B., Bronzino J. D., editors. Biomaterials principles and application. Boca Raton: CRC Press; 2003.

Saris, N.E.L., 2000. "Magnesium: An update on physiological, clinical and analytical aspects". Clinica Chimica Acta, Vol. 294, pp. 1-26.

Song, G., Atrens, A. Dargusch, M., 1999. "Influence of microstructure on the corrosion of diecast AZ91D", Corrosion Science, Vol. 41, pp. 249-273.

Staiger, M.P., Pietak, A.M., Huadmai, J. and Dias, G., 2006. "Magnesium and its alloys as orthopedic biomaterials: A review". Biomaterials, Vol. 27, pp. 1728-1734.

Turhan M.C., Lynch R., Killian M.S., Virtanen S., 2009. "Effect of acidic etching and fluoride treatment on corrosion performance in Mg alloy AZ91D (MgAlZn)", Electrochimica Acta, Vol. 55, pp. 250-257.

Wang, J.Y., Wicklund, B.H., Gustilo, R.B. and Tsukayama, D.T., 1996. "Titanium, chromium and cobalt ions modulate the release of bone-associated cytokines by human monocytes/macrophages *in vitro*". Biomaterials, Vol. 17, pp. 2233-2240.

Witte, F., Kaese, V., Hafferkamp, H., Switzer, E., Meyer-Lindenberg, A. and Wirth, C.J., 2005. "In vivo corrosion of four magnesium alloys and the associated bone response". Biomaterials, Vol. 26, pp. 3557-3563.

Zhang, T., Shao, Y., Meng, G., Cui, Z., Wang, F., 2011. "Corrosion of hot extrusion AZ91 magnesium alloy: I- relation between the microstructure and corrosion behaviour". Corrosion Science (in press), doi: 10.1016/jcorsci.2011.02.015.

Zhao M.-C., Liu M., Song G., Atrens A., 2008. "Influence of the β-phase on the corrosion of the Mg alloy AZ91", Corrosion Science, Vol. 50, pp. 1939-1953.

Zhou, W., Shen, T. and Aung, N.N., 2009. "Effect of heat treatment on corrosion behaviour of magnesium alloy AZ91D in simulated body fluid". Corrosion Science, Vol. 52, pp. 1035-1041.

7. RESPONSIBILITY NOTICE

The authors are the only responsible for the printed material included in this paper.